Dynamic Behavioral Modeling of 3G Power Amplifiers Using Real-Valued Time-Delay Neural Networks

Taijun Liu, Slim Boumaiza, *Student Member, IEEE*, and Fadhel M. Ghannouchi, *Senior Member, IEEE*

***Abstract*—In this paper, we propose a novel real-valued time-delay neural network (RVTDNN) suitable for dynamic modeling of the baseband nonlinear behaviors of third-generation (3G) base-station power amplifiers (PA). Parameters (weights and biases) of the proposed model are identified using the back-propagation algorithm, which is applied to the input and output waveforms of the PA recorded under real operation conditions. Time- and frequency-domain simulation of a 90-W LDMOS PA output using this novel neural-network model exhibit a good agreement between the RVTDNN behavioral model's predicted results and measured ones along with a good generality. Moreover, dynamic AM/AM and AM/PM characteristics obtained using the proposed model demonstrated that the RVTDNN can track and account for the memory effects of the PAs well. These characteristics also point out that the small-signal response of the LDMOS PA is more affected by the memory effects than the PAs large-signal response when it is driven by 3G signals. This RVTDNN model requires a significantly reduced complexity and shorter processing time in the analysis and training procedures, when driven with complex modulated and highly varying envelope signals such as 3G signals, than previously published neural-network-based PA models.**

***Index Terms*—Dynamic behavioral model, memory effects, power amplifier (PA), real-valued time delay neural network (RVTDNN), third-generation (3G) PAs.**

I. Introduction

SYSTEM-LEVEL behavioral modeling consists of constructing a black-box analytic function that admits alike responses to those obtained at the output of a real device or a subsystem driven by the same input signal. Such models are of great help for designers of communication systems, in particular, transmitters and power amplifiers (PAs) since they provide them with greatly reduced complexity and time-consuming design and optimization procedures. However, these advantages could be achieved providing the capacity of the model to predict the PA output under realistic conditions.

In the literature [1], the nonlinear behavioral models were classified as three categories: memoryless, quasi-memoryless behavioral models, and those with memory. Polynomial and Saleh [2] functions for a long while have been involved for solid-state and traveling-wave PAs modeling, respectively, that admit AM/AM and AM/PM conversion characteristics and belong to the first two categories. However, the continuously growing modulation bandwidth of the new communication multicarrier signals has triggered new challenging issues in the design of PAs due, namely, to memory effects. These effects are commonly defined as the frequency dependency of intermodulation-distortion levels at the output of PAs on the modulation frequency bandwidth [3]. In the time domain, memory effects cause the outputs of the small signals of the PA deviate from the linear output when the signal changes. This results in the deterioration of the whole system signal-to-noise ratio since the linearity of the PA at small signals is compromised.

Modeling of PAs with memory is the research focus of many authors over the last few years that yields to various model topologies. As an example, Schetzen [4] employed Volterra series for modeling nonlinear PAs with memory effects. However, the use of such series-based models is restricted to weak nonlinear devices. Solid-state power amplifiers (SSPAs) used in the third-generation (3G) base-station transceivers require high-order Volterra kernels. In spite of the fact that truncated Volterra series were pursued as a good means of getting rid of the computational complexity [5] of high-order Volterra kernels, this model still suffers from the difficulty of its real-time implementation. Jeckeln *et al.* [6] reported a cascade of a linear autoregressive moving average (ARMA) filter and a conventional polynomial memoryless function in order to take into account the frequency-dependent distortion at the output of the PA.

Traditionally, the extraction of the behavioral model parameters of PAs was performed with fitting the measured static AM/AM and AM/PM characteristics obtained using a power sweep continuous wave at the operation center frequency [2]. In order to handle the frequency response of the amplifier, Launay *et al.* [7] proposed to extract the behavioral model parameters by fitting static AM/AM and AM/PM characteristics at several carrier frequencies that fall within the signal bandwidth. This method was pursued as a solution to the modeling of PA driven with wide-band signals. However, this latter approach still suffers from the lack of accuracy since the static PA characterization technique was performed at each carrier frequency. Thus, Moulthrop *et al.* [8], Ku *et al.* [9], and Yang *et al.* [10] have chosen to extract model parameters while fitting concurrently measured amplitude and phase of the spectrum components at the PA output such as: 1) fundamentals; 2) third-order intermodulation (IMD3); and 3) fifth-order intermodulation (IMD5)

Manuscript received July 16, 2003; revised November 25, 2003. This work was supported by the National Sciences and Engineering Research Council of Canada.

The authors are with the Poly-Grames Research Center, Electrical Engineering Department, École Polytechnique de Montréal, Montréal, QC, Canada H3V 1A2 (e-mail: taijl@grmes.polymtl.ca; boumas@grmes.polymtl.ca; fadhel@grmes.polymtl.ca).

Digital Object Identifier 10.1109/TMTT.2004.823583

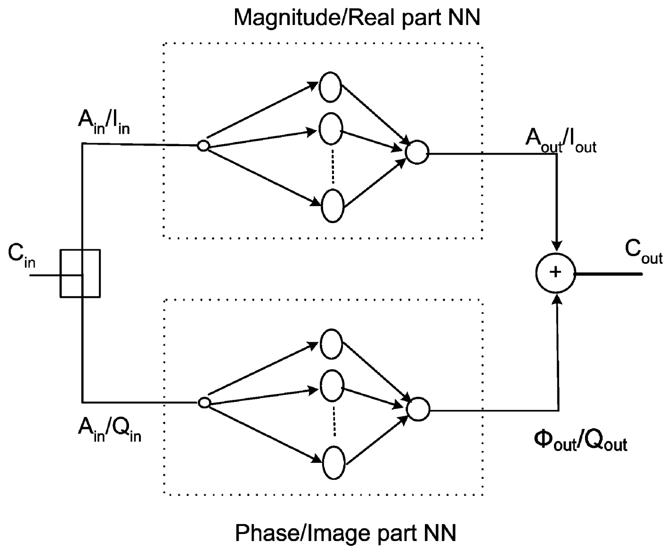

Fig. 1. Complex signal-processing models of the conventional real-valued neural network.

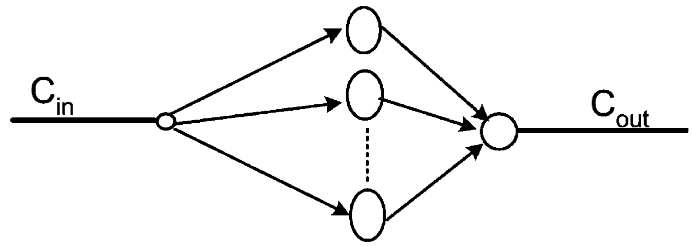

Fig. 2. Complex signal-processing models of the complex-valued neural network.

obtained under two-tone excitation signal with varying power and frequency spacing.

Over the last decade, artificial neural-network (ANN) technology has been successfully applied to RF and microwave applications [11] since they can approximate any continuous function arbitrarily well [12]. By profiting from their potential to learn the circuit behavior based on simulated or measured records of its input and output signals, they were used in nonlinear transient modeling and digital high-speed interconnects for computer-aided design (CAD) of very large scale integration (VLSI) modules [13]. They were also employed for the modeling, simulation, and design of microwave circuits [14]–[16]. Hence, the ANN-based models are seen as a potential alternative to model RF PAs having medium-to-strong memory effects along with high-order nonlinearity. This paper represents an attempt to further extend the use of neural-network technology to the dynamic modeling of RF PAs of wireless communication transmitters operating under wide-band modulation and highly varying envelope signals such as CDMA 2000, W-CDMA, TD-SCDMA, and WLAN802.11x.

II. RVTDNN Behavioral Model of PAs

Many topologies of ANNs were reported in the literature for the modeling of different types of circuits and systems that exhibit different kinds of linear and nonlinear behaviors. In conventional ANN model development procedures, complex input–output measured signals are initially converted to either a polar representation (magnitude and phase) or rectangular one (in-phase I and quadrature Q components). Then, two separate and uncoupled real-valued neural networks are used to model the output amplitude and phase (or the output I and Q components) variations as a function of the input power amplitude (or the input I and Q components), as shown in Fig. 1 [17]. The real coefficients of the two networks are identified during a training procedure using the measured amplitude and phase (or I and Q components) of the input and output. This topology suffers from the convergence problems of the training procedure since the two networks are trained separately. Furthermore, Benvenuto *et al.* [18] and Ibnkahla and Castanie [19] proposed applying a complex-value-based neural network to the complex signal directly, as shown in Fig. 2. In such a case, both the weights and activation functions of the network are complex. This type of ANN necessitates a cumbersome complex training algorithm such as the complex back-propagation training algorithm [20]. Thus, the two neural-network topologies described above lead to a lengthy training time and elevated computation resources.

As a specific ANN, the time-delay neural network (TDNN) has been used to learn and represent dynamic systems. It was successfully utilized in signal processing, speech recognition, system identification, and control to solve the temporal processing problems [12], [21]. However, in the case of complex input signals, the TDNN was implemented according to the topologies of Figs. 1 or 2. Therefore, it suffers from the limitations mentioned earlier. In this paper, we propose a novel real-valued time delay neural network (RVTDNN) to construct a dynamic behavioral model suitable for 3G PAs in real operation conditions. Contrary to previous presented methods, this approach uses only one real-valued neural network instead of two separate networks. The newly proposed RVTDNN, which is made up of two layers, uses real-valued parameters (weights and biases) along with the real components of the input and output signals. As shown in Fig. 3, the RVTDNN model utilizes the two components of the input signal ($I_{\rm in}$, $Q_{\rm in}$) in order to predict the correspondent two components ($I_{\rm out}$, $Q_{\rm out}$) of the output signal. The proposed RVTDNN is based on the feed-forward neural network (FFNN) [22], with the addition of two tapped delay lines (TDLs) in its two baseband inputs. TDLs are used so as to consider the history of the input signal, which is needed for memory effects modeling. Thus, the FFNN entries include not only the current value of the input signal, but also its previous ones. The memory depth of the device-under-test (DUT) will be reflected on the length of the TDL taps. Consequently, the TDL structure, included in the RVTDNN, leads to the modeling of the short-term memory effects exhibited by the PA. However, the long-term memory is built into the RVTDNN through a supervised learning. This kind of long-term memory can be used to simulate the slow dynamic changes of nonlinear characteristics of the PA over time.

Considering the memory effects of the PA, the baseband output $I_{\rm out}$ and $Q_{\rm out}$ components of the PA at instant n are a function of p past value of the baseband input $I_{\rm in}$ and q past

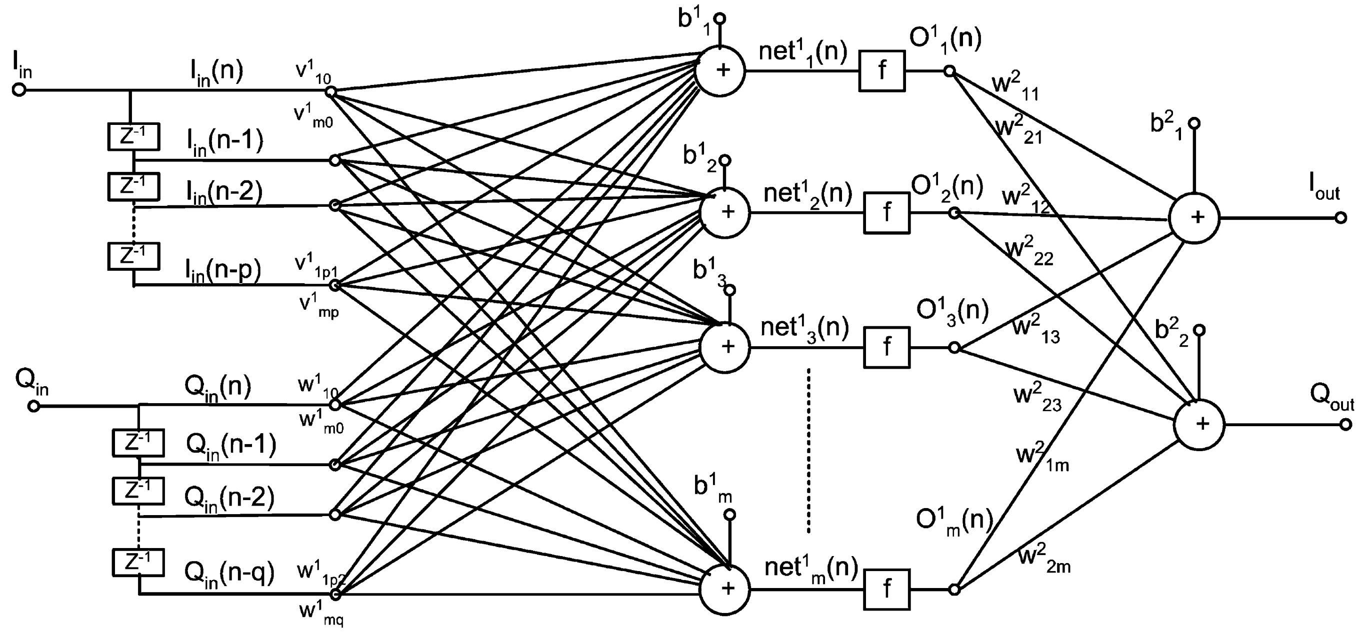

Fig. 3. Block diagram of new two-layer RVTDNN PA behavioral model.

values of the baseband input $Q_{\rm in}$ according to (1) and (2) as follows:

$$I_{\rm out}(n) = f_I\big[I_{\rm in}(n), I_{\rm in}(n-1), \ldots, I_{\rm in}(n-p), Q_{\rm in}(n), Q_{\rm in}(n-1), \ldots, Q_{\rm in}(n-q)\big] \quad (1)$$

$$Q_{\rm out}(n) = f_Q\big[I_{\rm in}(n), I_{\rm in}(n-1), \ldots, I_{\rm in}(n-p), Q_{\rm in}(n), Q_{\rm in}(n-1), \ldots, Q_{\rm in}(n-q)\big]. \quad (2)$$

Based on the RVTDNN shown in Fig. 3, (1) and (2) can be rewritten as follows:

$$I_{\rm out}(n) = \sum_{k=1}^{m} w_{1k}^2 O_k^1(n) + b_1^2 \quad (3)$$

$$Q_{\rm out}(n) = \sum_{k=1}^{m} w_{2k}^2 O_k^1(n) + b_2^2 \quad (4)$$

where

$$O_k^1(n) = f\left(\text{net}_k^1(n)\right) \quad (5)$$

and

$$\text{net}_k^1(n) = \sum_{i=0}^{p} v_{ki}^1 I_{\rm in}(n-i) + \sum_{i=0}^{q} w_{ki}^1 Q_{\rm in}(n-i) + b_k^1 \quad (6)$$

$k = 1, 2, \ldots m$ and $f(x) = \tanh(x) = (1-e^{-2x})/(1+e^{-2x})$ is the activation function.

When $p = q = 0$, i.e., the length of the TDL is zero. The RVTDNN then regresses to a real-valued feed-forward neural network (RVFFNN) and, hence, it will be limited to a memoryless or quasi-memoryless model.

III. Extraction of RVTDNN Behavioral Model Parameters

Parameter extraction of the RVTDNN model commonly denoted as a learning procedure is performed with fitting the measured input and output I and Q components. Furthermore, as one observes in Fig. 3, the RVTDNN model can be converted to a common FFNN or multilayer perceptron (MLP) with $p+q+2$ inputs and two outputs. Thus, the dynamic problem becomes a static problem and the standard back-propagation training algorithm [12] can be employed to train it. The algorithm adjusts the network parameters so as to minimize the cost function E, over an epoch, defined as follows:

$$E = \sum_{n=1}^{N} E_n = \frac{1}{2N} \sum_{n=1}^{N} \left[\left(I_{\rm out}(n) - \hat{I}_{\rm out}(n)\right)^2 + \left(Q_{\rm out}(n) - \hat{Q}_{\rm out}(n)\right)^2 \right] \quad (7)$$

where E_n is the instantaneous error. $I_{\rm out}(n)$ and $Q_{\rm out}(n)$ represent the outputs of RVTDNN at instant n, and $\hat{I}_{\rm out}(n)$ and $\hat{Q}_{\rm out}(n)$ are the desired outputs at instant n. N denotes the length of the training sequence.

In this study, the training procedure of the real-valued neural network is performed based on a realistic dynamic characterization of an amplifier under test fed with a modulated input signal instead of one- or two-tone signals. Thus, the characterization of the PA is made without any induction of self-heating effects due to signal excitation as the case of continuous-wave-based measurement techniques. Moreover, the behavioral model will yield to enhanced prediction accuracy since its parameters are identified using characterization data captured when the DUT is fed with a modulated input signal that implies a real operation condition. Experiments conducted for the training and validation of the neural network used a real-time two-channel time-domain sampling system. $I_{\rm in}$ and $Q_{\rm in}$ components of the equivalent complex baseband input signal of the PA are used as two independent inputs of the RVTDNN. The RVTDNN also has two outputs corresponding to $I_{\rm out}$ and $Q_{\rm out}$ components of the equivalent complex baseband output signal, respectively.

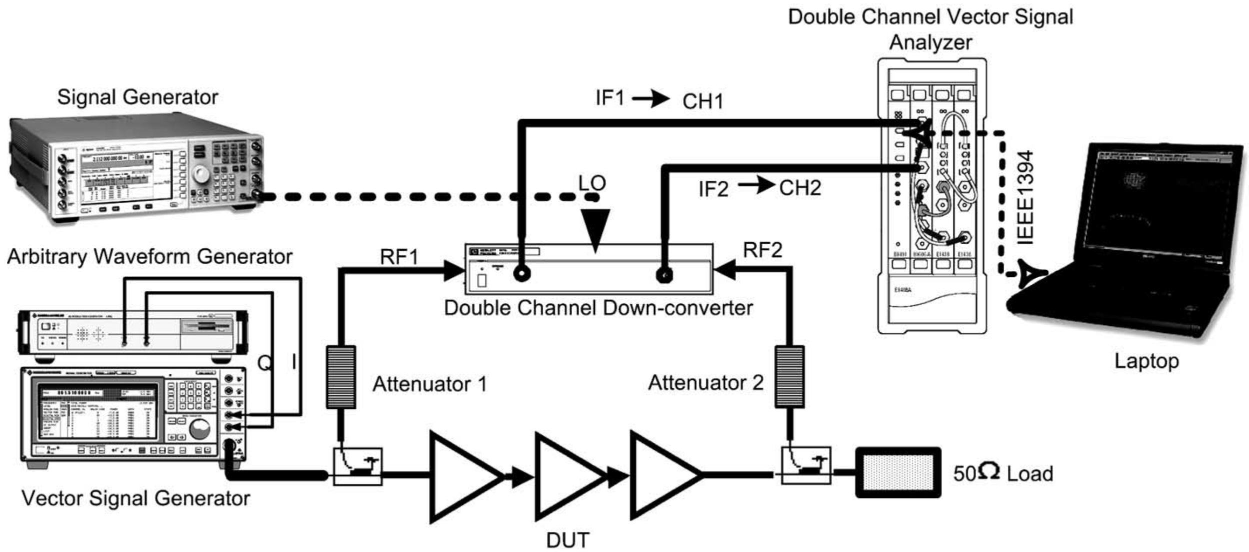

Fig. 4. Accurate complex behavioral test-bed block diagram.

TABLE I
TRAINING AND VALIDATION SIGNAL CHARACTERISTICS

Signal	IS95	CDMA2000-SR3	Three-carrier CDMA2000-SR3
Frequency bandwidth	1.2288 MHz	3.6864 MHz	13.6864 MHz
Crest Factor	10.73	9.70 dB	12.75 dB

In such a way, measured I and Q components of the complex baseband input and output signals are directly exploited to train the RVTDNN.

The initialization of the network is an important issue for training the RVTDNN with the back-propagation algorithm. The initial weights were chosen randomly from a suitable range, such as $(-0.8,\ 0.8)$. They were uniformly distributed inside this range and are symmetric around zero. After the RVTDNN training procedure converges, the RVTDNN model parameters are found. Since the model is derived directly from the time-domain sampled data emerging for the PA driven by the real signal, it is possible to update the model parameters when the performance of the PA changes due to any internal or external factors or important changes in the nature and/or statistics of the driving signal.

Once the RVTDNN is trained, all of the model parameters are known and it becomes the dynamic behavioral model of the PA. The generality is an important specification to evaluate the performance of the trained neural-network model. Good generality requires that the neural network must perform well on a new test data set distinct from the one used in the training sequence. Thus, a very small value of the cost function reached by the trained network does not imply that a good model is obtained and it can generalize well to new inputs. Moreover, it has been observed, during this study, that excessive training on the training sequence decreases occasionally the performance on the test data. This phenomenon, called over-fitting, could

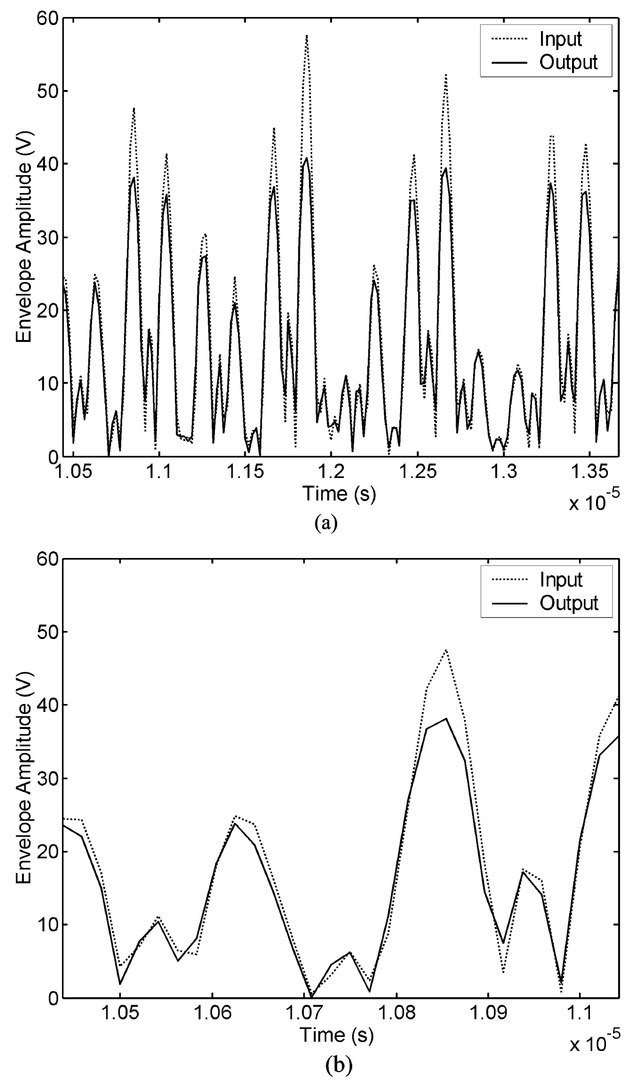

Fig. 5. Envelope waveforms of the three-carrier CDMA2000 signal. (a) Normalized input and output signals magnitude versus time. (b) Zoom-in of the input and output waveforms.

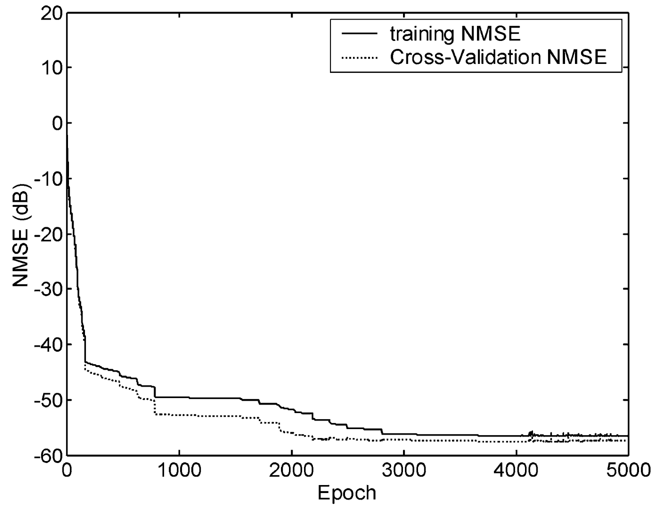

Fig. 6. Typical convergence curve of the training process.

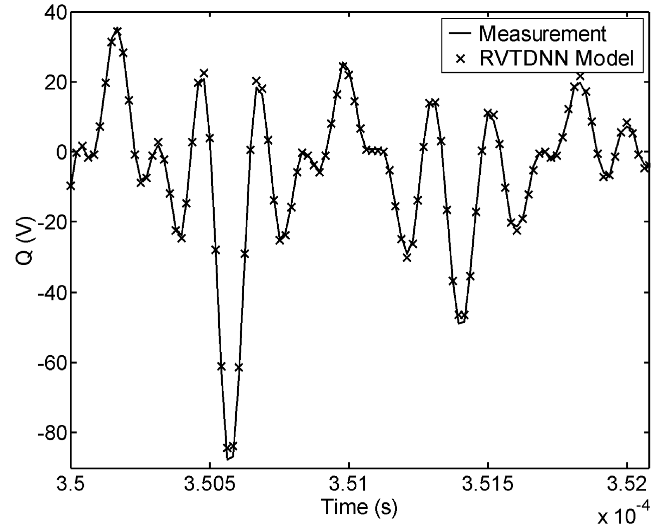

Fig. 8. Validation results of the Q component in the time domain.

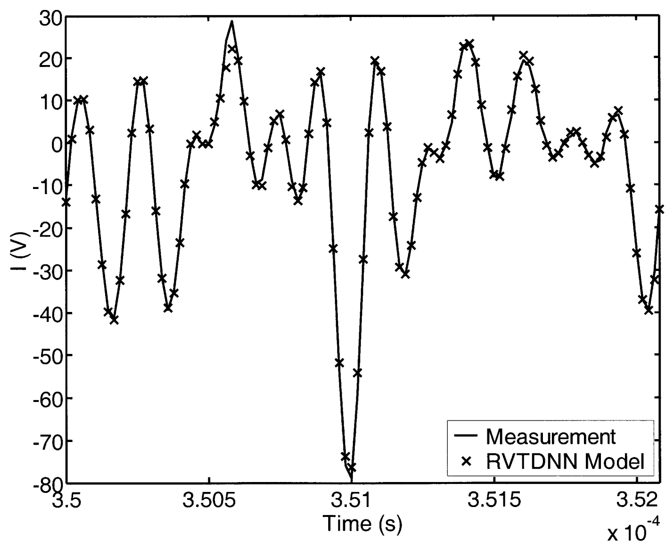

Fig. 7. Validation results of the I component in the time domain.

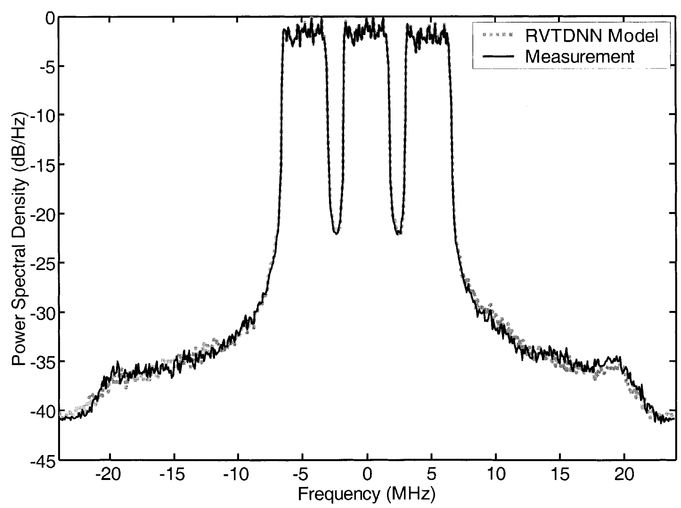

Fig. 9. PSD comparison between the RVTDNN behavioral model and the measurement data of the three-carrier CDMA2000 signal.

be avoided through a constant evaluation of the network using a set of test data, i.e., making cross-validation, as learning proceeds. If there is a succession of training epoch in which performance improves only for the training data and not for the test data, over-fitting is considered to have occurred and the training process should be terminated. Hence, the learning process should be controlled carefully so as to obtain good performance neural-network behavioral models of PAs.

IV. Measurements of Baseband Data of a 3G PA

A 90-W peak class AB LDMOS PA [23] was used in this study for model validation purposes. It is a three-stage PA suitable for a 3G wireless base-station transmitter operating at a 1930–1990-MHz band. The overall small-signal gain of the lineup is 58 dB. The PA peak output power at 1-dB gain compression is approximately 49 dBm.

The baseband I and Q waveforms at the input and output of the DUT needed in the different steps of this study were captured using the complex behavior PA instantaneous characterization test bed shown in Fig. 4 [23], [24]. For that, the vector signal generator (SMIQ) in combination with the (I/Q) arbitrary waveform generator (AMIQ) was used for generating test signals. These signals are synthesized using the software WinIQSIM (version 3.6) from Rohde and Schwarz, Munich, Germany, and Advanced Design System from Agilent Technologies, Palo Alto, CA. RF signals at the input and output of the DUT are first translated, in the frequency domain, to an intermediate frequency using a double-channel down-converter. The IF1 and IF2 outputs of the down-converter feed the two channels of the baseband vector signal analyzer (VSA) 89610B. The dynamic range of this dual-channel receiver is better than 70 dB. A laptop in this test bed is used to run the vector signal analysis software for the acquisition of the two-channel waveform signals. The delay calibration function of the VSA is exploited to compensate for the time-delay lag between the receiver's two channels caused by the group delay of the DUT.

The system described above was used to collect the instantaneous baseband input and output signals for training and validation purposes of the RVTDNN. Three tests signals were used

TABLE II
COMPARISON OF TRAINING PERFORMANCES FOR RVFFNN AND RVTDNN

Model	RVFFNN		RVTDNN	
Method	Training	Cross-Validation	Training	Cross-Validation
MSE	5.01×10^{-4}	4.64×10^{-4}	1.39×10^{-4}	1.14×10^{-4}
NMSE	1.81×10^{-2}	1.71×10^{-2}	5.03×10^{-3}	3.98×10^{-3}
R	0.99736	0.99778	0.99748	0.99802

for validation purposes of the RVTDNN model, i.e.: 1) an IS 95 signal; 2) a one-carrier CDMA-2000-SR3 signal; and 3) a three-carrier CDMA-2000-SR3 signal. All these signals have been synthesized with the ADS CDMA2000 library. Table I gives the main characteristics of these signals. The crest factors of the synthesized signals are defined at 0.001% of the complementary cumulative probability density function (CCPDF). Fig. 5 shows the envelope waveforms of the three-carrier CDMA2000-SR3 signal at the input and output of the PA, where the input signal was multiplied by the small-signal gain of the PA. The gain compression can be easily seen in Fig. 5(a). The variation of small-signal gain due to memory effects can be illustrated as shown in Fig. 5(b).

V. RVTDNN MODEL: TRAINING AND VALIDATION RESULTS

A. Training and Validation of the RVTDNN Model With Three-Carrier CDMA2000-SR3 Signal

A two-layer RVTDNN, as shown in Fig. 3, was used to illustrate the performance of this behavioral model. It contained two neurons in the input and output layers, respectively. The number of neurons in the hide layer and the number of taps in the two input TDLs were determined by an optimization program. An RVTDNN model having 15 neurons and five taps was found, through an optimization procedure, to be appropriate for the LDMOS PA driven by 3G signals.

Ten-thousand (10K) sample data from the three-carrier CDMA-2000-SR3 measurements were used to train the RVTDNN. Five-thousand (5K) sample data from measurements at another period of time were used to make cross-validation during the training process to ensure the generality of the model. Thirty-thousand (30K) sample data from other period of measurements were used to test the behavioral model trained.

Fig. 6 shows a typical convergence curve of the RVTDNN training process using a three-carrier CDMA-2000-SR3 signal. The test set of the validation data (30K data), which had never been used during a training process, was used to validate the model obtained. Figs. 7 and 8 show the time-domain validation results of I and Q components of the neural behavioral model for a three-carrier CDMA-2000-SR3 signal. The behavioral model matches the measurement data well even though the validation data have never been used in training. Therefore, one can state that the extracted RVTDNN model exhibits good generality for the three-carrier CDMA2000 signal. The power spectral density (PSD) comparison between the results of the RVTDNN behavioral model and the measurement results is shown in Fig. 9. It demonstrates that the RVTDNN behavioral model also has good performance in the frequency domain.

B. Dynamic AM/AM and AM/PM Curves for RVTDNN and RVFFNN Models

In order to demonstrate the merit of the proposed RVTDNN model, a conventional RVFFNN model is utilized to characterize the equivalent baseband behavior of the PA. The output of an RVFFNN is dependent only on the inputs at the same instantaneous. The RVFFNN has two layers, in which there are 15 neurons in the hide layer and two neurons in the input and output layers. These two models were trained using a three-carrier CDMA-2000-SR3 signal. The training performance for RVFFNN and RVTDNN models are listed in Table II, in which the mean square error (MSE), normalized mean square error (NMSE), and the correlation coefficient (R) are represented [25] respectively. Based on Table II, both of the correlation coefficient R obtained for the two kinds of neural-network models are higher than 0.997 ($\cong$1). This suggests that outputs of these two models almost co-vary with the measurement data, which means that they vary nearly by the same amount with the measurement data for both networks. However, one can clearly observe that the proposed RVTDNN model offers better accuracy than the RVFFNN one since it allows a lower value of the MSE and NMSE in the prediction of the PA output.

With the time-domain validation results of the RVFFNN and RVTDNN behavioral models, the comparison between the dynamic AM/AM and AM/PM characterizations of the behavioral models and those of the measurement data can easily be given, as shown in Figs. 10 and 11, respectively. Herein, the measured dynamic AM/AM and AM/PM conversion characteristics are no longer smooth curves as those we see generally for a memoryless/quasi-memoryless PA. These kinds of deviation reveal the time-dependent relations of the outputs to the inputs of 3G PAs. It is this time-dependent relation that stands for the memory effects of 3G PAs. The outputs of the 3G PAs, corresponding to the inputs with same amplitudes, will vary at different instantaneous. As we anticipated, the RVTDNN behavioral model represents the memory effects (time-dependent effects) of the PA. However, the RVFFNN model cannot express this kind of time-dependent effects of the PA and it is only a statistical mean result because the RVFFNN's structure determines that the RVFFNN will try to learn the average between different outputs when the current inputs are the same.

The dynamic AM/AM and AM/PM characteristics also suggest that the small-signal response of the PA is strongly affected by the memory effects for 3G applications contrary to the PA's large-signal response, which is caused by the high peak-to-average ratio of 3G signals. At first view, this looks strange

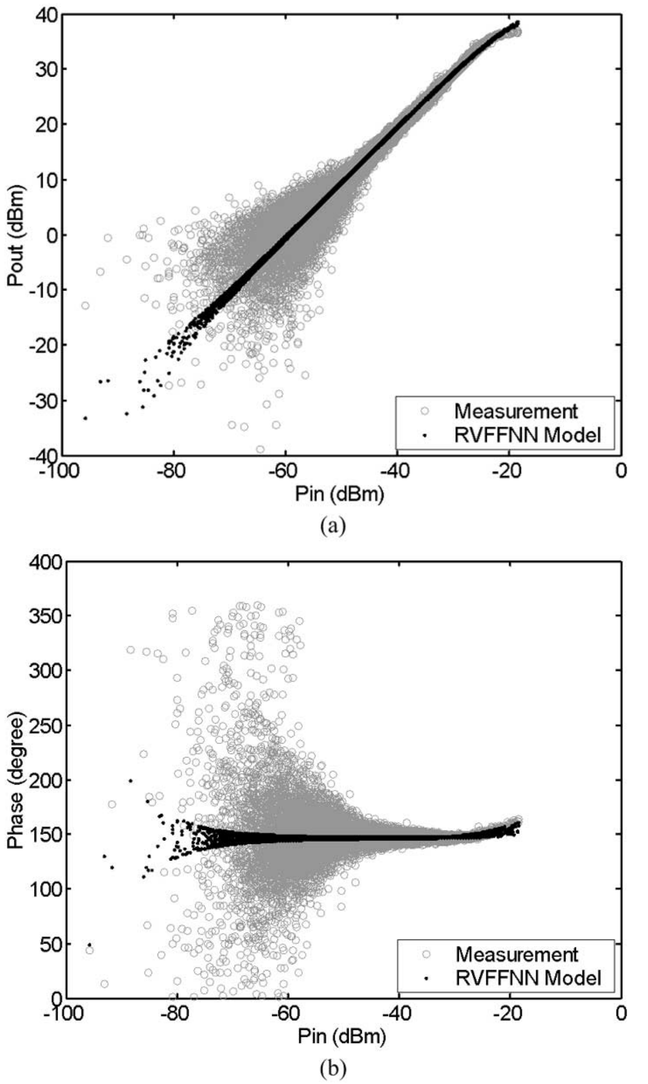

Fig. 10. Dynamic AM/AM and AM/PM characteristic comparison between the RVFFNN behavioral model and measurement data. (a) Dynamic AM/AM characteristics. (b) Dynamic AM/PM characteristics.

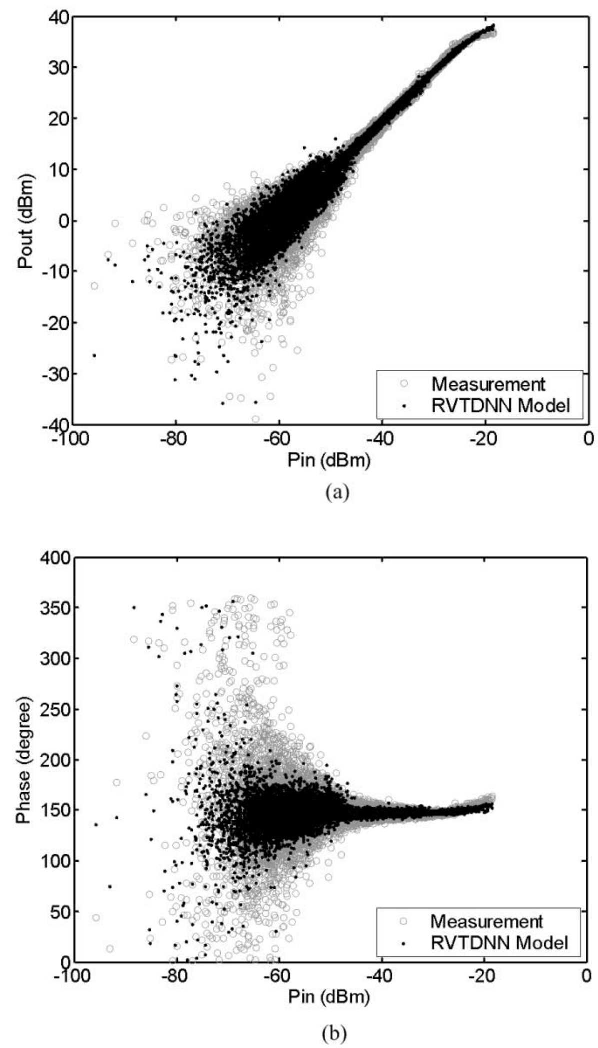

Fig. 11. Dynamic AM/AM and AM/PM characteristic comparison between the RVTDNN behavioral model and the measurement data. (a) Dynamic AM/AM characteristics. (b) Dynamic AM/PM characteristics.

since the traditional narrow-band system with constant envelope signals should present linear properties for small signals, i.e., there is no AM/AM and AM/PM conversion for small signals. However, for nonconstant envelope signals applied to 3G PAs, the output of a small signal will be strongly affected by the nearby previous large signals because of the memory effects. The relative variation (scattering) range of the small signals is larger than that of the large signal. It is easy to see that this kind of relative variation becomes larger and larger with the signal becoming smaller and smaller from the measured AM/AM and AM/PM conversion characteristics. This is in agreement with the results previously published in [6].

C. Validation With IS95 and CDMA-2000-SR3 Signals

With the purpose of proving the effectiveness of the RVTDNN model for other signals, a one-carrier CDMA2000 signal was used to train the same RVTDNN, as described above. A different set of data of the one-carrier CDMA2000 signal and a new set of data of the IS95 signal, which was never used before, were applied to the RVTDNN model obtained.

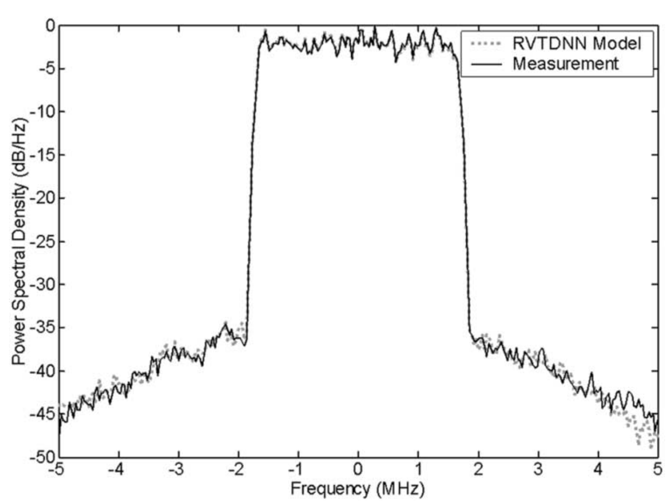

Fig. 12. PSD comparison between the RVTDNN behavioral model and the measurement data of the one-carrier CDMA2000 signal.

Figs. 12 and 13 show the PSD comparison between the results predicted by the RVTDNN model and the measurement results

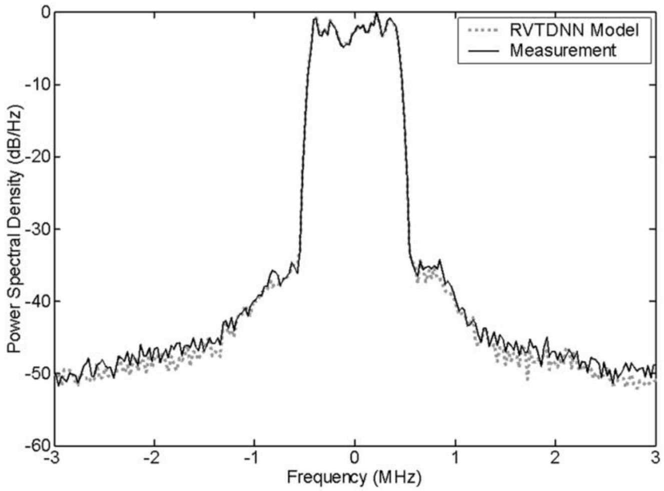

Fig. 13. PSD comparison between the RVTDNN behavioral model and the measurement data of the IS95 signal.

for both signals. Even though the IS95 signal was not used to train the RVTDNN, the validation still gave satisfactory results. Hence, the RVTDNN model does have good generality for similar signals having close statistical characteristics and it is back-compatible with signals having a smaller bandwidth.

VI. Conclusion

In this paper, a RVTDNN that has the capability to learn and predict the dynamic behavior of nonlinear PAs has been proposed. This real-valued neural-network model largely reduces the complexity of the neural network in the presence of complex modulated signals having highly time-varying envelopes. The back-propagation algorithm is used to train the neural network so as to extract the model parameters. Validation and accuracy assessment of the developed RVTDNN model in the time domain showed an agreement between the RVTDNN behavioral model output data and measurement ones for 3G signals. The frequency-domain validation of the model also showed a good agreement between the PA's output spectrum calculated using the RVTDNN model predicted waveforms and the measured spectrum for IS 95, one-carrier CDMA2000-SR3, and three-carrier CDMA2000-SR3 signals.

The dynamic AM/AM and AM/PM simulation results point out that the RVTDNN can account for the memory effects (time-dependent effects) of the LDMOS PA very well. Moreover, the dynamic AM/AM and AM/PM characteristics also suggest that the small-signal response of the LDMOS PA is strongly affected by the memory effects for 3G applications. The satisfactory validation results of the IS95 signal, which was applied to an RVTDNN model trained by a one-carrier CDMA2000-SR3 signal, has proven that the RVTDNN model obtained does have good generality for similar signals having close statistical characteristics and crest factors. In such a case, the RVTDNN model shows it is back compatible and can be used to predict the response of the PA with signals having smaller modulation bandwidth.

Acknowledgment

The authors would like to acknowledge J. Gauthier and R. Archambault, both of the École Polytechnique de Montréal, Montréal, QC, Canada, for providing technical and software supports during measurements.

References

[1] K. Hyunchui, M. D. Mckinley, and J. S. Kenney, “Extraction of accurate behavioral models for power amplifiers with memory effects using two-tone measurements,” in *IEEE MTT-S Int. Microwave Symp. Dig.*, vol. 1, June 2002, pp. 139–142.

[2] M. C. Jeruchim, P. Balaban, and K. S. Shanmugan, *Simulation of Communication Systems: Modeling, Methodology, and Techniques*. New York: Kluwer, 2000.

[3] J. H. K. Vuolevi, T. Rahkonen, and J. P. A. Manninen, “Measurement technique for characterizing memory effects in RF power amplifiers,” *IEEE Trans. Microwave Theory Tech.*, vol. 49, pp. 1383–1389, Aug. 2001.

[4] M. Schetzen, *The Volterra and Wiener Theories Nonlinear Systems*. New York: Wiley, 1980.

[5] A. Zhu, M. Wren, and T. J. Brazil, “An efficient Volterra-based behavioral model for wideband RF power amplifiers,” in *IEEE MTT-S Int. Microwave Symp. Dig.*, vol. 2, June 2003, pp. 787–790.

[6] E. G. Jeckeln, S. Huei-Yuan, E. Martony, and M. Eron, “Method for modeling amplitude and bandwidth dependent distortion in nonlinear RF devices,” in *IEEE MTT-S Int. Microwave Symp. Dig.*, vol. 3, June 2003, pp. 1733–1736.

[7] F. Launay, Y. Wang, S. Toutain, S. T. D. Barataud, J. M. Nebus, and R. Quere, “Nonlinear amplifier modeling taking into account HF memory frequency,” in *IEEE MTT-S Int. Microwave Symp. Dig.*, vol. 2, June 2002, pp. 865–868.

[8] A. A. Moulthrop, C. J. Clark, C. P. Silva, and M. S. Muha, “A dynamic AM/AM and AM/PM measurement technique,” in *IEEE MTT-S Int. Microwave Symp. Dig.*, June 1997, pp. 1455–1458.

[9] H. Ku, M. D. McKinley, and J. S. Kenney, “Quantifying memory effects in RF power amplifiers,” *IEEE Trans. Microwave Theory Tech.*, vol. 50, pp. 2843–2849, Dec. 2002.

[10] Y.Youngoo Yang, J. Yi, J. Nam, and B. Kim, “Behavioral modeling of high power amplifiers based on measured two-tone transfer characteristics,” *Microwave J. (Euro-Global Edition)*, vol. 43, pp. 90–104, Dec. 2000.

[11] Q. J. Zhang and K. C. Gupta, *Neural Networks for RF and Microwave Design*. Norwood, MA: Artech House, 2000.

[12] S. Haykin, *Neural Networks: A Comprehensive Foundation*. Upper Saddle River, NJ: Prentice-Hall, 1999.

[13] Y. Cao, J. J. Xu, V. K. Devabhaktuni, R. T. Ding, and Q. J. Zhang, “An adjoint dynamic neural network technique for exact sensitivities in nonlinear transient modeling and high-speed interconnect design,” in *IEEE MTT-S Int. Microwave Symp. Dig.*, vol. 1, June 2003, pp. 165–168.

[14] J. J. Xu, M. C. E. Yagoub, R. T. Ding, and Q. J. Zhang, “Neural-based dynamic modeling of nonlinear microwave circuits,” *IEEE Trans. Microwave Theory Tech.*, vol. 50, pp. 2769–2780, Dec. 2002.

[15] Y. H. Fang, M. C. E. Yagoub, F. Wang, and Q. J. Zhang, “A new macromodeling approach for nonlinear microwave circuits based on recurrent neural networks,” *IEEE Trans. Microwave Theory Tech.*, vol. 48, pp. 2335–2344, Dec. 2000.

[16] J. W. Nandler, M. A. Ismail, J. E. Rayas-Sanchez, and Q. J. Zhang, “New directions in model development for RF/microwave components utilizing artificial neural networks and space mapping,” in *IEEE MTT-S Int. Microwave Symp. Dig.*, vol. 4, 1999, pp. 2572–2575.

[17] M. Ibnkahla, J. Sombrin, F. Castanie, and N. J. Bershad, “Neural networks for modeling nonlinear memoryless communication channels,” *IEEE Trans. Commun.*, vol. 45, pp. 768–771, July 1997.

[18] N. Benvenuto, F. Piazza, and A. Uncini, “A neural network approach to data predistortion with memory in digital radio systems,” in *Proc. IEEE Int. Communications Conf.*, vol. 1, Singapore, Nov. 1995, pp. 152–156.

[19] M. Ibnkahla and F. Castanie, “Vector neural networks for digital satellite communications,” in *Proc. IEEE Int. Communications Conf.*, vol. 3, Seattle, WA, June 1995, pp. 1865–1869.

[20] H. Leung and S. Haykin, “The complex backpropagation algorithm,” *IEEE Trans. Signal Processing*, vol. 39, pp. 2101–2104, Sept. 1991.

[21] Y. Bengio, *Neural Networks for Speech and Sequence Recognition*. New York: ITC Press, 1995.

[22] I. W. Sandberg, *Nonlinear Dynamical Systems: Feedforward Neural Network Perspectives*. New York: Wiley, 2001.
[23] S. Boumaiza and F. M. Ghannouchi, "An accurate complex behavior test bed suitable for 3G power amplifiers characterization," in *IEEE MTT-S Int. Microwave Symp. Dig.*, vol. 3, June 2002, pp. 2241–2244.
[24] ——, "Realistic power-amplifiers characterization with application to baseband digital predistortion for 3G base stations," *IEEE Trans. Microwave Theory Tech.*, vol. 50, pp. 3016–3021, Dec. 2002.
[25] J. C. Principe, N. R. Euliano, and W. C. Lefebvre, *Neural and Adaptive Systems: Fundamentals Through Simulations*. New York: Wiley, 2000.

Taijun Liu received the B.S. degree in applied physics from the University of Petroleum (East China), Dongying, China, in 1986, the M.Eng. degree in electrical engineering from the University of Electronic Science and Technology of China, Chengdu, China, in 1989, and is currently working toward the Ph.D. degree at the École Polytechnique de Montréal, Montreal, QC, Canada.

From 1989 to 1992, he was a Lecturer with the Chongqing University of Posts and Telecommunications, Chongqing, China. From 1992 to 1998, he was a Senior Engineer with the Dianqiangui Petroleum Exploration Bureau, Information Technology Company, Kunming, China. From 1999 to 2000, he was a Software Engineer with ElectromagneticWorks Inc., Montreal, QC, Canada. Since September 2000, he has been with the École Polytechnique de Montréal. His current research interests are digital signal processing, neural networks, nonlinear modeling, and linearization of wide-band PAs.

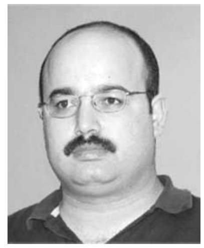

Slim Boumaiza (S'00) received the B.Eng. degree in electrical engineering from the École Nationale des Ingénieurs de Tunis, Tunis, Tunisia, in 1997, the M.Sc.A. degree from the École Polytechnique de Montréal, Montréal, QC, Canada, in 1999, and is currently working toward the Ph.D. degree at the École Polytechnique de Montréal.

His current research interests are design, linearization, characterization and modeling of high-power and spectrum-efficient RF amplifiers.

Fadhel M. Ghannouchi (S'84–M'88–SM'93) received the B.Eng. degree in engineering physics and the M.S. and Ph.D. degrees in electrical engineering from the École Polytechnique de Montréal, Montréal, QC, Canada, in 1983, 1984, and 1987, respectively.

He is currently a Professor with the Département de génie électrique, École Polytechnique de Montréal, where he has taught electromagnetics and microwave theory and techniques since 1984. He has provided consulting services to a number of microwave companies. He is also the founder of AmpliX Inc., Montréal, QC, Canada, a company that offer linearization products and services to wireless and satcom equipment manufacturers. His research interests are in the areas of microwave/millimeter-wave instrumentation and measurements, nonlinear modeling of microwave active devices, and design of power and spectrum efficient microwave amplification systems.

Dr. Ghannouchi is a Registered Professional Engineer in the Province of Quebec, Canada. He has served on the Technical Committees of several international conferences and symposiums.